THE JOURNAL OF BIOLOGICAL CHEMISTRY VOL. 287, NO. 30, pp. 25292–25302, July 20, 2012

Nickel-induced Epithelial-Mesenchymal Transition by Reactive Oxygen Species Generation and E-cadherin Promoter Hypermethylation*[S]

Received for publication, August 9, 2011, and in revised form, May 29, 2012 Published, JBC Papers in Press, May 30, 2012, DOI 10.1074/jbc.M111.291195

Chih-Hsien Wu[‡], Sheau-Chung Tang[‡], Po-Hui Wang[‡§], Huei Lee[‡], and Jiunn-Liang Ko[‡¶1]

From the [‡]Institute of Medicine, Chung Shan Medical University and the Departments of [§]Obstetrics and Gynecology and [¶]Medical Oncology and Chest Medicine, Chung Shan Medical University Hospital, Taichung 40203, Taiwan

Background: Epithelial-mesenchymal transition (EMT) is an important program in tumor metastasis.
Results: Nickel chloride ($NiCl_2$) induced EMT in human bronchial epithelial cells, including down-regulation of epithelial-cadherin (E-cadherin) and up-regulation of fibronectin.
Conclusion: ROS generation and promoter hypermethylation of E-cadherin are involved in $NiCl_2$-mediated EMT.
Significance: The results of this study may shed new light on the role of nickel in carcinogenesis.

Epithelial-mesenchymal transition (EMT) is considered a critical event in the pathogenesis of lung fibrosis and tumor metastasis. During EMT, the expression of differentiation markers switches from cell-cell junction proteins such as E-cadherin to mesenchymal markers such as fibronectin. Although nickel-containing compounds have been shown to be associated with lung carcinogenesis, the role of nickel in the EMT process in bronchial epithelial cells is not clear. The aim of this study was to examine whether nickel contributes to EMT in human bronchial epithelial cells. We also attempted to clarify the mechanisms involved in $NiCl_2$-induced EMT. Our results showed that $NiCl_2$ induced EMT phenotype marker alterations such as up-regulation of fibronectin and down-regulation of E-cadherin. In addition, the potent antioxidant *N*-acetylcysteine blocked EMT and expression of HIF-1α induced by $NiCl_2$, whereas the DNA methyltransferase inhibitor 5-aza-2′-deoxycytidine restored the down-regulation of E-cadherin induced by $NiCl_2$. Promoter hypermethylation of E-cadherin, determined by quantitative real time methyl-specific PCR and bisulfate sequencing, was also induced by $NiCl_2$. These results shed new light on the contribution of $NiCl_2$ to carcinogenesis. Specifically, $NiCl_2$ induces down-regulation of E-cadherin by reactive oxygen species generation and promoter hypermethylation. This study demonstrates for the first time that nickel induces EMT in bronchial epithelial cells.

Epithelial mesenchymal transition (EMT)[2] is the biological process by which cells switch from polarized immotile epithelial type to motile mesenchymal type. The processes of EMT include reorganization of the actin cytoskeleton, remodeling of epithelial cell-cell and cell-matrix adhesion contacts, repression of epithelial markers (*e.g.* epithelial-cadherin and E-cadherin), induction of mesenchymal markers (*e.g.* fibronectin), and acquisition of motile capacity. EMT has been primarily described in embryonic development and organ formation. Nevertheless, recent studies have demonstrated an association between the EMT process and cancer progression. This process is considered a transient and reversible event that can lead to tumor progression (1, 2). Inhibition of the EMT process in cancer cells results in reduced tumor invasion and metastatic spread, indicating that this is an important therapeutic target for cancer therapy (3–5).

E-cadherin is a cell surface adhesion glycoprotein that plays an important role in EMT-mediated cancer cell progression (6). DNA deletion, mutational inactivation, gene silencing, and proteolytic degradation contribute to the loss of E-cadherin expression during tumor progression (4, 7). Accumulated hypoxia-inducible factor-1α (HIF-1α), a key mediator of cellular adaptation to hypoxia, and up-regulated Snail and Slug repress E-cadherin expression and E-cadherin tumor malignancy (5, 8). Moreover, epigenetic inhibition of E-cadherin by promoter hypermethylation following chronic exposure to low doses of cigarette smoke condensate has been reported *in vitro* (9). Various pathways in the regulation of E-cadherin might inhibit the EMT process. We attempted to determine the key pathway for inhibiting the EMT process in our tumor model.

DNA damage induced by metal compounds (*e.g.* nickel, arsenic, lead, chromium, manganese, and cadmium) promotes ROS production in carcinogenesis (10). Nickel and several of its compounds are widely used in modern industry. The International Agency for Research on Cancer classifies metallic nickel and nickel compounds as possibly carcinogenic and carcinogenic to humans, respectively (10). High consumption of nickel products leads to exposure to nickel via air, soil, food, water, tobacco smoke, and occupational and environmental pollution (11). Significantly higher nickel concentrations in lung tissues of lung cancer patients, in comparison with normal controls, suggest that nickel contributes to lung carcinogenesis *in vivo*.

* This work was supported by National Science Council, Taiwan, Grant NSC-99-2314-B-040-012-MY3.
[S] This article contains supplemental Figs. S1–S3.
[1] To whom correspondence should be addressed: Institute of Medicine, Chung Shan Medical University, 110, Section 1, Chien-Kuo N. Rd., Taichung 40203, Taiwan. Tel.: 886-4 24730022-11694; Fax: 886-4 24751101; E-mail: jlko@csmu.edu.tw.
[2] The abbreviations used are: EMT, epithelial-mesenchymal transition; ROS, reactive oxygen species; SOD, superoxide dismutase; NAC, *N*-acetylcysteine; QMSP, quantitative real time methyl-specific PCR; HPF, 3′-(*p*-hydroxyphenyl) fluorescein.

Recently, it has been found that soluble nickel ions interact with cell surface receptors and disrupt active cell signaling, resulting in induction of genes, such as *HIF-1α* (12). This indicates that nickel contributes to the EMT process in lung cancer. We hypothesized that nickel compounds induce EMT and increase malignancy during lung carcinogenesis. To test this hypothesis, we treated bronchial epithelial BEAS-2B cells with nickel chloride ($NiCl_2$) and found that $NiCl_2$ induces EMT. In addition, we demonstrated that repression of E-cadherin by $NiCl_2$ is involved in ROS induction and aberrant methylation of *E-cadherin* promoter.

EXPERIMENTAL PROCEDURES

Cell Lines and Chemicals—Human bronchial epithelial cell lines (BEAS-2B cells) immortalized with SV40 (American Type Culture Collection, Manassas, VA) were maintained in serum-free LHC-9 medium (BioSource International Inc., Nivelles, Belgium) in an incubator at 37 °C in a humidified atmosphere of 5% CO_2. $NiCl_2$ (Sigma, N-6136), nickel sulfate ($NiSO_4$, Sigma, N-4882), sodium arsenite ($NaAsO_2$, Sigma, S-7400), *N*-acetylcysteine (NAC, Sigma, A-7250), deferoxamine mesylate (Sigma, D9533), and 5-aza-2′-deoxycytidine (Sigma, A-3656) were obtained from Sigma.

Immunofluorescence—BEAS-2B cells were seeded onto 24-well plates (2×10^5 cells/well) with coverslips and treated with $NiCl_2$ (0, 0.25, and 0.5 mM) for 72 h. Next, the cells were fixed and incubated with primary antibody against human E-cadherin (BD Biosciences, 610182) at 4 °C overnight. This was followed by incubation with secondary antibody goat anti-mouse FITC (A11011, Alexa Fluor® 488) for 60 min after washing with PBS. Thereafter, cells were stained with DAPI (1:1000) for 45 min. E-cadherin was detected on a confocal laser scanning microscope (Zeiss LSM 510 META) at 630× magnification.

Western Blot Analysis—Anti-fibronectin (BD Biosciences, 610077), anti-E-cadherin (BD Biosciences, 610182), anti-Snail (Cell Signaling, 3879S), anti-Slug (Cell Signaling, 9585S), anti-HIF-1α (BD Biosciences, 610959), anti-NADPH oxidase 1 (NOX1) (GeneTex Inc., GTX103888), anti-SOD2 (Santa Cruz Biotechnology, sc-18503), anti-catalase (GeneTex Inc., GTX110704), anti-glutathione peroxidase-1/2 (GPX-1/2) (Santa Cruz Biotechnology, sc-133160), and anti-β-actin (Sigma, A5441) antibodies were used to detect fibronectin, E-cadherin, Snail, Slug, HIF-1α, SOD2, catalase, GPX-1/2, and β-actin, respectively. The complete protocol for Western blot analysis has been described previously (13).

Isolation of RNA, Reverse Transcriptase-PCR, and Quantitative Real Time-PCR Analysis—Total RNA was isolated using TRIzol reagent (Invitrogen). The combinational DNA was then reverse-transcribed from 2 μg of total RNA using random hexamer primers and Moloney murine leukemia virus reverse transcriptase, RNase H minus (Promega). For fibronectin, the primers were 5′-CCGTGGGCAACTCTGTC-3′ (forward) and 5′-TGCGGCAGTTGTCACAG-3′ (reverse); for E-cadherin, the primers were 5′-TGGAGAGACACTGCCAACTG-3′ (forward) and 5′-AGGCTGTGCCTTCCTACAGA3′ (reverse); and for β-actin, the primers were 5′-TCATCACCATTGGCAATGAG-3′ (forward) and 5′-CACTGTGTTGGCGTACAGGT-3′ (reverse). Real time-PCR was performed using an ABI PRISM 7000 real time PCR system with gene-specific primers and Taqman Universal PCR Master Mix, No AmpErase UNG (Applied Biosystems). Glyceraldehyde-3-phosphate dehydrogenase served as the internal control.

Detection of ROS by Flow Cytometry and Fluorescence Spectroscopy—BEAS-2B cells were pretreated with or without 10 mM NAC for 1 h. This was followed by treatment with $NiCl_2$ and staining with 10 μM 2′,7′-dichlorodihydrofluorescein diacetate (D399), 10 μM 3′-(*p*-aminophenyl) fluorescein (Invitrogen, A36003), 10 μM 3′-(*p*-hydroxyphenyl) fluorescein (HPF, Invitrogen, H36004), or 10 μM dihydroethidium (Invitrogen, D1168) for 30 min. The cells were harvested and washed twice with PBS, resuspended in PBS, and analyzed by flow cytometry. Ethidium fluorescence was measured using fluorescence spectroscopy (excitation 485 nm and emission 590 nm).

Mitochondrial Membrane Potential Measurement—Mitochondrial membrane potential levels were measured using lipophilic cation 5,5′,6,6′-tetrachloro-1,1′,3,3′-tetraethylbenzimidazolcarbocyanine iodide 1 (JC-1) fluorescent dye (Invitrogen, T3168). The cells were plated and treated as indicated, and 1 μM JC-1 was added 30 min prior to harvest. Cells were collected by trypsinization and washed with PBS. The red (aggregated JC-1; R2 region) and green (monomeric JC-1; R1 region) fluorescence signals were analyzed by flow cytometry (BD Biosciences) and Cell Quest software (BD Biosciences).

RNA Interference—RNAi reagents were obtained from the National RNAi Core Facility of the Institute of Molecular Biology/Genomic Research Center, Academia Sinica. Individual clones were identified by their unique TRC number, *e.g.* shLuc TRCN0000072246 for vector control targeted to luciferase and shHIF-1α (810) and TRCN0000003810 (responding sequence, GTGATGAAAGAATTACCGAAT) for vector targeted to HIF-1α. The cells were selected using 2 μg/ml puromycin (Sigma, P8833).

Chromatin Immunoprecipitation (ChIP) Assay—ChIP assay was carried out according to the manufacturer's protocol (chromatin immunoprecipitation assay kit, catalog no. 17-295, Upstate Biotechnology Inc., Lake Placid, NY). Immune complexes were prepared using anti-HIF-1α (BD Biosciences, 610959) or anti-Snail (Cell Signaling, 3879S) antibody. The supernatant of immunoprecipitation reaction carried out in the absence of antibody served as the total input DNA control. PCR was carried out with 10 μl of each sample using the following primers: *E-cadherin* promoter-S, 5′-CTGGTACCTCCAGGCTAGAGGGTCACCG-3′; *E-cadherin* promoter-AS, 5′-TTAAAGCTTCCGGGTGCGGTCGGGTCGGG-3′. This was followed by analysis on 2% agarose gels. Primers from the *E-cadherin* open reading frame for amplification of a 270-bp fragment served as the PCR control.

Methylation-specific PCR—Genomic DNA was isolated using the genomic DNA isolation kit (Qiagen, Inc., Hilden, Germany). Bisulfite treatment was carried out as described previously (14). Methylation patterns within the *E-cadherin* CpG island of exon 1 (sequence −126 bp to +144 bp relative to transcription start site, GenBank™ accession number D49685) were determined using a previously described nested PCR approach (15). The sequencing primers were 5′-GTTTAGTT-

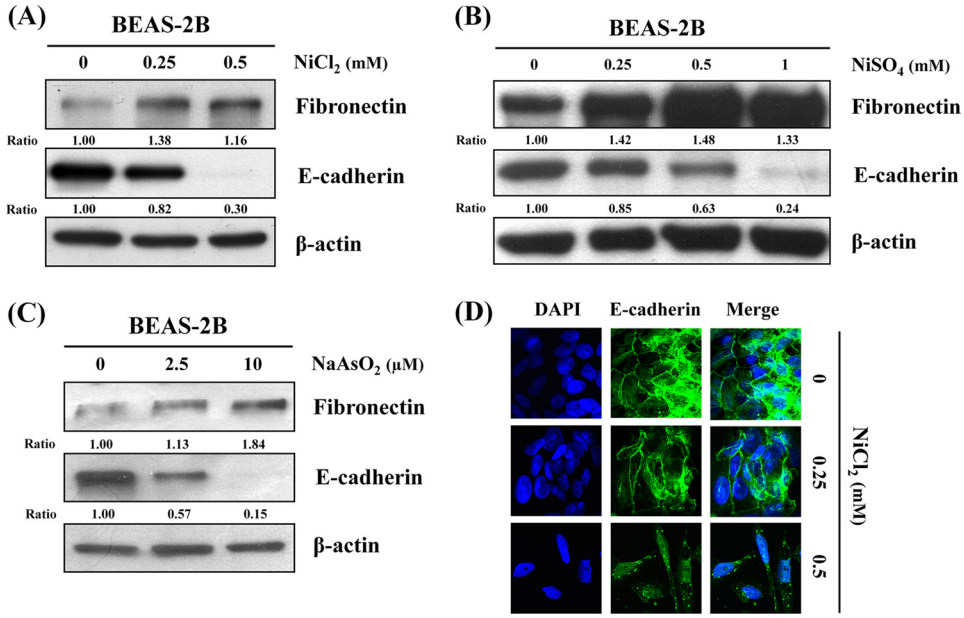

FIGURE 1. **Protein levels of EMT marker in metal compound-treated human BEAS-2B cells.** BEAS-2B cells (1×10^6 cells/6-cm dish) were treated with the nickel chloride ($NiCl_2$) 0, 0.25, and 0.5 mM (*A*); nickel sulfate ($NiSO_4$) 0, 0.25, 0.5, and 1 mM (*B*); or sodium arsenite ($NaAsO_2$) 0, 2.5, 10 μM for 72 h (*C*); and protein levels of fibronectin and E-cadherin were detected by Western blot. β-Actin was used as the internal control. The relative ratios of fibronectin/β-actin and E-cadherin/β-actin are shown. *D,* $NiCl_2$ (0, 0.25, and 0.5 mM) for 72 h and immunofluorescence staining for E-cadherin (*green*) plus DAPI counterstaining for DNA (*blue*). Original magnification, ×630.

TTGGGGAGGGGTT-3′ (sense) and 5′-ACTACTACTCCA-AAAACCCATAACTAA-3′ (antisense). The cycling conditions consisted of an initial denaturation step at 95 °C for 5 min, followed by the addition of 1 unit of *Taq* polymerase and 30 cycles at 95 °C for 30 s, 50 °C for 30 s, and 72 °C for 30 s. Nested primer sequences for E-cadherin for the methylated reaction were 5′-TGTAGTTACGTATTTATTTTTAGTGGCGTC-3′ (sense) and 5′-CGAATACGATCGAATCGAACCG-3′ (antisense). The primer sequences for the unmethylated reaction were 5′-TGGTTGTAGTTATGTATTTATTTTTAGTGGT-GTT-3′ (sense) and 5′-ACACCAAATACAATCAAATCAAA-CCAAA-3′ (antisense). PCR parameters were the same as those listed above, except that the annealing temperatures for the methylated and unmethylated reactions were 64 and 62 °C, respectively. The product sizes of the methylated and unmethylated reactions were 112 and 120 bp, respectively.

Quantitative Real Time Methylation-specific PCR—Semi-quantitative methylation specific PCR (QMSP) was carried out with Smart Quant Green Master Mix kit (Protech Technology, Taiwan) and primers specific for fully methylated *E-cadherin* promoter sequences (16). Real time-PCR conditions were 95 °C for 15 min followed by 45 cycles at 94 °C for 15 s and 60 °C for 1 min with data acquisition after each cycle. Triple replicates of each sample were obtained by laser detector of ABI Prism 7000 sequence detection system. C_T values of each sample were determined.

Bisulfate Genomic Sequencing—Modified DNA was amplified with two rounds of PCR using two pairs of nested primers. First round PCR was performed using primer S1 5′-TTTTGA-TTTTAGGTTTTAGTGAGTTAT-3′ (upstream, sequence position −277 to −250) and primer S2 5′-AATACCTACAA-CAACAACAACAA-3′ (downstream, +177 to +154). Amplification for PCR was performed with ProTaq polymerase (Protech Technology, Taiwan) under the following PCR conditions (94 °C for 2 min and 35 cycles at 94 °C for 20 s, 52 °C for 20 s, and 72 °C for 30 s, with a final extension at 72 °C for 5 min). For the second round of PCR, nested primers S3 5′-TGTAGGTTTT-ATAATTTATTTAGATTT-3′ (upstream, −211 to −184) and S4 5′-ACTCCAAAAACCCATAACTAAC-3′ (downstream, +138 to +116) were used. The PCR conditions were 94 °C for 2 min with 30 cycles at 94 °C for 30 s, 54 °C for 30 s, and 72 °C for 45 s, followed by an extension at 72 °C for 5 min. The PCR products were purified and inserted into vector pGEM-T Easy Vector System (A3610; Promega) using Fast DNA Ligation System (Promega). Five clones from each cell line or tissue were sequenced to assess the level of methylation at each CpG site, as described previously (17).

RESULTS

Metal Compounds Induce EMT in BEAS-2B Cells—To investigate whether metal compounds induce EMT in lung carcinogenesis and fibrosis, we analyzed the effects of $NiCl_2$, $NiSO_4$, and $NaAsO_2$ on E-cadherin and fibronectin expressions in BEAS-2B cells. After exposure to these compounds for 72 h, the expressions of epithelial marker E-cadherin decreased 70, 76, and 85%, respectively. In contrast, the expressions of mesenchymal marker fibronectin increased 1.16-, 1.33-, and 1.84-fold at the highest doses, respectively (Fig. 1, *A–C*). The EMT process for the E-cadherin complex on the lateral plasma membrane in untreated BEAS-2B cells is described on immunofluorescence assay in Fig. 1*D*. Expression of E-cadherin was significantly reduced, and cells underwent morphological changes following $NiCl_2$ treatment (Fig. 1*D*). To better understand the role of nickel compounds in the EMT process, we selected $NiCl_2$ for further validation experiments.

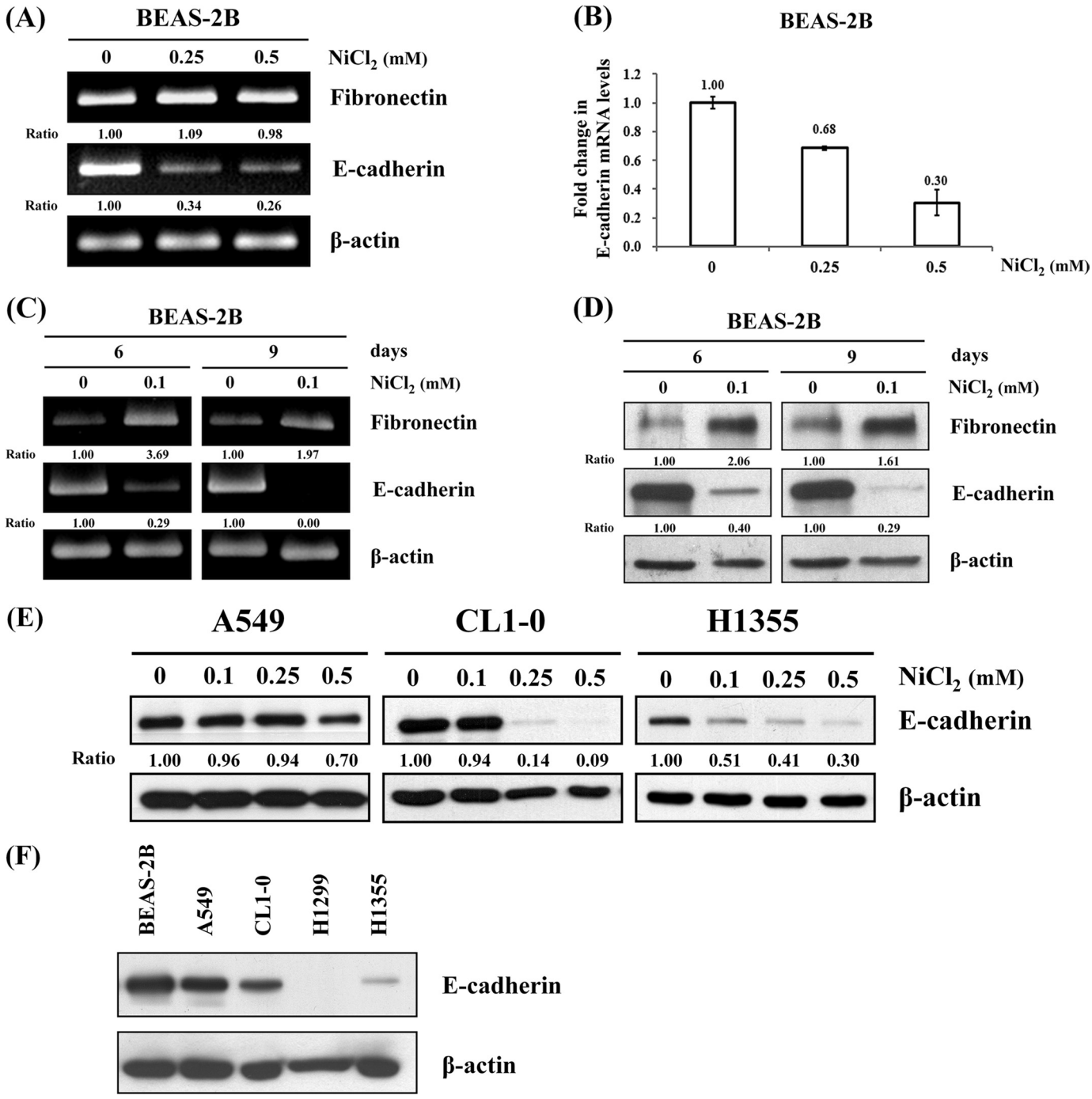

FIGURE 2. **Effects of $NiCl_2$ on EMT in BEAS-2B cells.** *A,* BEAS-2B cells (1×10^6 cells/6-cm dish) were treated with $NiCl_2$ (0, 0.25, and 0.5 mM) for 48 h, and mRNA levels of fibronectin and E-cadherin were determined on RT-PCR. β-Actin was used as the internal control. The relative ratios of fibronectin/β-actin and E-cadherin/β-actin are shown. *B,* quantitative real time PCR analysis was used to detect E-cadherin expression with total RNA extracted from cells treated with $NiCl_2$ (0, 0.25, and 0.5 mM) for 48 h. All values have been normalized to the level of GAPDH and are the averages of three independent readings. *C,* during the time course study, BEAS-2B cells were exposed to $NiCl_2$ (0 and 0.1 mM) for the indicated times. The EMT marker expressions were analyzed on RT-PCR (*D*) and Western blot. β-Actin was used as the internal control. The relative ratios of fibronectin/β-actin and E-cadherin/β-actin are shown. *E,* A549, CL1-0, and H1355 lung cancer cells (5×10^5 cells/6-cm dish) were treated with $NiCl_2$ (0, 0.1, 0.25, and 0.5 mM) for 72 h, and the protein levels of E-cadherin were detected on Western blot. β-Actin was used as the loading control. The relative ratios of E-cadherin/β-actin are shown. *F,* protein levels of E-cadherin in BEAS-2B, A549, CL1-0, H1299, and H1355 cells. Thirty μg of total proteins were loaded onto each lane for Western blot analysis. β-Actin was used as the internal control.

$NiCl_2$ Induces Dose- and Time-dependent EMT in BEAS-2B Cells—To assess the mRNA expressions of EMT markers in $NiCl_2$-treated BEAS-2B cells, cells were treated with 0, 0.25, or 0.5 mM $NiCl_2$ for 48 h and analyzed by RT-PCR. As shown in Fig. 2*A*, E-cadherin mRNA levels were down-regulated 66 and 74% in BEAS-2B cells treated with $NiCl_2$ at 0.25 and 0.5 mM, respectively, when compared with untreated cells. However, fibronectin mRNA was not up-regulated by $NiCl_2$. The same results were obtained using real time RT-PCR for the detection of mRNA expression of E-cadherin in BEAS cells treated with $NiCl_2$ (Fig. 2*B*). The results revealed that E-cadherin is repressed by $NiCl_2$ at transcriptional levels.

In general, humans are exposed to low doses of nickel compounds via air pollution. To explore the effect of long term low dose exposure to $NiCl_2$ on human lung cells, BEAS-2B cells were treated with low dose (0.1 mM) $NiCl_2$ for various times (6 and 9 days). The expression of E-cadherin decreased and that of fibronectin increased (Fig. 2, *C* and *D*). These results demonstrated that long term low dose exposure to $NiCl_2$ promotes the EMT process in bronchial epithelial cells. In addition, to assess whether $NiCl_2$ represses expression of E-cadherin in lung cancer cell lines, A549, CL1-0, and H1355 cells were treated with various concentrations of $NiCl_2$. As shown in Fig. 2*E*, the expression of E-cadherin slightly decreased in A549 cells but dramatically decreased in CL1-0 and H1355 cells. These results further support the role of $NiCl_2$ in promoting lung cancer EMT. We also found that the protein levels of E-cadherin in BEAS-2B, A549, and CL1-0 cells were higher than in H1299 and H1355 cells in the untreated state (Fig. 2*F*).

ROS Mediates $NiCl_2$-induced EMT—It has been well documented that nickel exposure leads to generation of ROS and activation of signaling pathways by activating transcription factor (18). BEAS-2B cells were pretreated with different antioxidants or ROS inhibitors/scavengers, including NAC (antioxidant), Tiron (superoxide anion scavenger), superoxide dismutase (SOD), allopurinol (xanthine oxidase inhibitor), and rotenone (mitochondria respiratory chain inhibitor). As shown in Fig. 3*A*, NAC, Tiron, and SOD all abolished $NiCl_2$-induced EMT. NAC was able to simultaneously diminish up-regulation of fibronectin and restore E-cadherin expression in the presence of $NiCl_2$.

To further confirm this finding, cells were pretreated with 10 mM NAC and then treated with various concentrations of $NiCl_2$. This resulted in the mitigation of $NiCl_2$-mediated down-regulation of E-cadherin and up-regulation of fibronectin and HIF-1α (Fig. 3*B*). Intracellular nickel competes with iron for iron- binding sites on enzymes and proteins (19). Free iron can increase ROS formation, which may be important during ROS-associated EMT (20). To investigate whether free iron promotes $NiCl_2$-induced EMT, we co-treated cells with $NiCl_2$ and deferoxamine mesylate, an iron chelator. Results showed that $NiCl_2$ reduces E-cadherin and up-regulates fibronectin after deferoxamine mesylate co-treatment, indicating that intracellular free iron ions are not involved in $NiCl_2$-induced EMT (Fig. 3*C*).

Metals can induce DNA damage either directly or indirectly through the formation of ROS (21). To determine whether $NiCl_2$ induces specific ROS production, cells were treated with various ROS-sensitive probes using flow cytometry. The generation of ROS by $NiCl_2$ was detected by photocatalysis using 2′,7′-dichlorodihydrofluorescein diacetate, 3′-(*p*-aminophenyl) fluorescein, and HPF. Pretreatment of cells with 10 mM NAC for 1 h significantly blunted the ROS production after $NiCl_2$ treatment (Fig. 4*A* and supplemental Fig. S1*A*). However, there was no apparent alteration in superoxide anion generation. To confirm these results, antimycin A was used as a positive control to induce superoxide production. Superoxide levels increased in comparison with untreated cells after antimycin A treatment (Fig. 4*B* and supplemental Fig. S1*B*). However, $NiCl_2$ did not induce superoxide generation in a time course study.

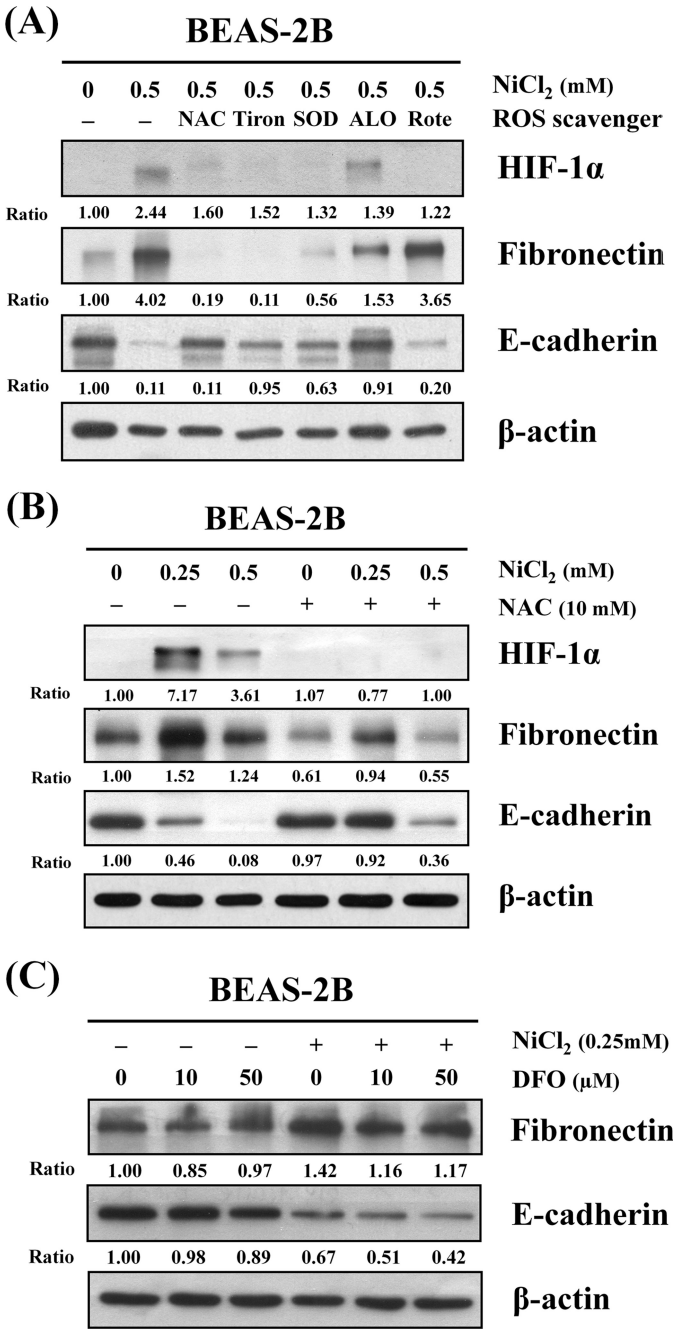

FIGURE 3. **ROS are involved in $NiCl_2$-induced EMT.** *A*, BEAS-2B cells (1×10^6 cells/6-cm dish) were preincubated with 10 mM NAC, 10 mM Tiron, 500 units/ml SOD, 200 μM allopurinol (*ALO*), or 1 μM rotenone (*Rote*) for 1 h followed by culture with or without 0.5 mM $NiCl_2$ for 72 h. *B*, BEAS-2B cells were pretreated with 10 mM NAC for 1 h followed by exposure to $NiCl_2$ (0, 0.25, and 0.5 mM) for 72 h. *C*, BEAS-2B cells were treated with $NiCl_2$ (0 and 0.25 mM, respectively) with or without desferrioxamine (*DFO*) (0, 10, and 50 μM) for 72 h. The protein levels were determined on Western blot analysis. β-Actin was used as the internal control. The relative ratios of HIF-1α/β-actin, fibronectin/β-actin, and E-cadherin/β-actin are shown.

Rather, the levels of superoxide decreased following $NiCl_2$ treatment for 72 h (Fig. 4*B*). Next, we assessed the effects of antioxidant enzymes on Ni-induced EMT. Catalase and GPX1/2 were down-regulated, whereas NOX1 and SOD2 were up-regulated by $NiCl_2$ (Fig. 4*C*). In addition, we measured the changes in mitochondrial membrane potential in $NiCl_2$-treated BEAS-2B cells. Treatment with 0.5 mM $NiCl_2$ con-

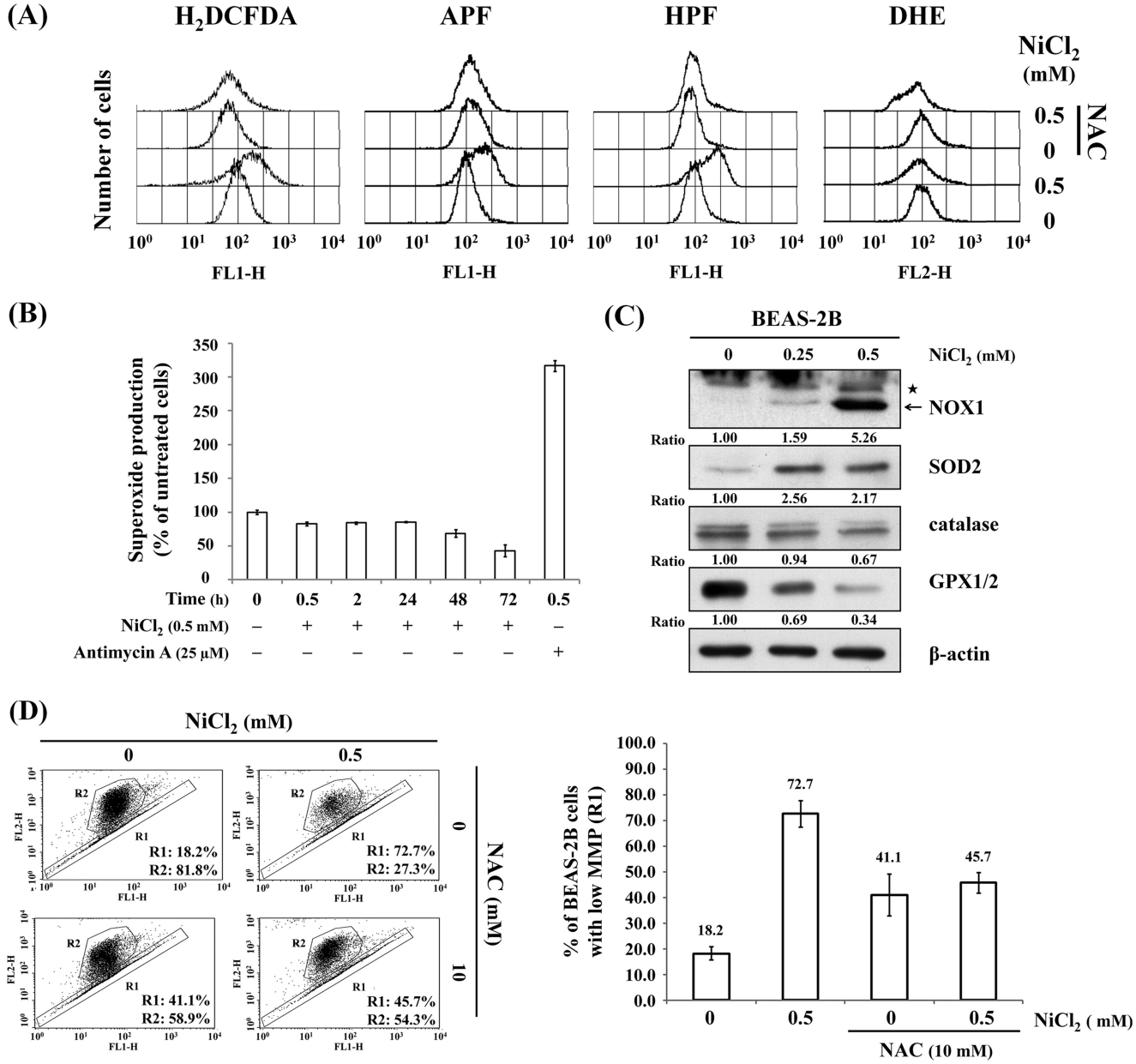

FIGURE 4. **$NiCl_2$ induces ROS generation.** *A*, BEAS-2B cells (1×10^6 cells) were pretreated with 10 mM NAC for 1 h followed by exposure to 0.5 mM $NiCl_2$ for 72 h. The cells were stained with 10 μM 2′,7′-dichlorodihydrofluorescein diacetate (ROS indicator), 10 μM 3′-(*p*-aminophenyl) fluorescein (hypochlorite anion indicator), 10 μM (HPF hydroxyl radical indicator), or 10 μM dihydroethidium (superoxide anion indicator) dye and analyzed by flow cytometry. *B*, cells were treated with 0.5 mM $NiCl_2$ for 0.5, 2, 24, 48, and 72 h or 25 μM antimycin A for 30 min (positive control). Superoxide anion production was measured by ethidium fluorescence generated from dihydroethidium (10 μM) by fluorescence spectroscopy and expressed as the percentage of untreated cells. *C*, cells were treated with 0, 0.25, and 0.5 mM $NiCl_2$ for 72 h, and protein levels of NADPH oxidase 1 (*NOX1*), SOD2, catalase, and glutathione peroxidase (*GPX1/2*) were detected on Western blot. β-Actin was used as the internal control. *Asterisk* represents a nonspecific band. The relative ratios of NOX1/β-actin, SOD2/β-actin, catalase/β-actin, and GPX1/2/β-actin are shown. *D*, BEAS-2B cells were untreated/treated with 0.5 mM $NiCl_2$ as well as 0 or 10 mM NAC for 72 h. The changes in mitochondrial membrane potential (*MMP*) were assessed by the intensity of green fluorescence (*R1*) and red fluorescence (*R2*) of JC-1. *Bar graph* shows the quantification changes in JC-1 fluorescence in the presence of $NiCl_2$ with/without NAC co-treatment as detected on flow cytometry assay. There was interaction between $NiCl_2$ and NAC with $NiCl_2$ decreasing JC-1 fluorescence in the presence of NAC. Data are presented as mean ± S.E.

verted JC-1 from aggregate form (R2) to monomer form (R1), indicating a disruption in mitochondrial function (18.2% *versus* 72.7%). $NiCl_2$-mediated mitochondrial apoptotic pathway was restrained in NAC-pretreated cells (Fig. 4*D*).

HIF-1α, Snail, and Slug Are Involved in $NiCl_2$-mediated Inhibition of E-cadherin—HIF-1α is produced during exposure to arsenite through the generation of ROS in arsenite-induced carcinogenesis (22). Therefore, we hypothesized that $NiCl_2$ induces EMT by aberrant activation of HIF-1α signaling. HIF-1α was markedly up-regulated after $NiCl_2$ stimulation (Fig. 5*A*), indicating that $NiCl_2$ down-regulation of E-cadherin is mediated by HIF-1α. To clarify the role of HIF-1α in $NiCl_2$-diminished expression of E-cadherin, HIF-1α silencing experiment was carried out with VZV-G pseudotyped lentivirus-shRNA system. The responses of BEAS-2B shLuc cells to $NiCl_2$ treatment were similar to those of parental BEAS-2B cells. E-cadherin was partially restored, and fibronectin did not increase following exposure to $NiCl_2$ in BEAS-2B shHIF1-α

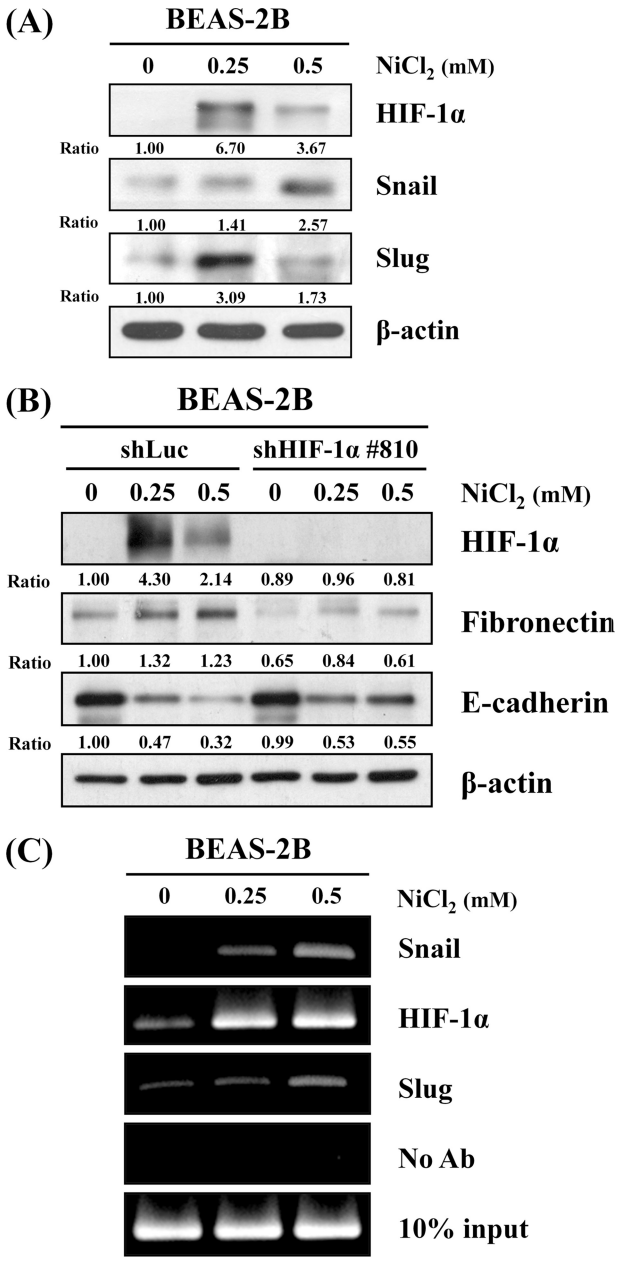

FIGURE 5. **HIF-1α, Snail, and Slug are involved in nickel-induced EMT.** *A,* Western blot analysis shows HIF-1α, Snail, and Slug expressions in protein lysates from BEAS-2B cells (1×10^6 cells) treated with $NiCl_2$ at the indicated dosages for 72 h. β-Actin was used as the internal control. The relative ratios of HIF-1α/β-actin, Snail/β-actin, and Slug/β-actin are shown. *B,* HIF-1α, fibronectin, and E-cadherin protein levels were determined on Western blot using protein lysates from cells treated with $NiCl_2$ for 72 h after infection with lentivirus carrying shHIF-1− or vector control. β-Actin was used as the internal control. The relative ratios of HIF-1α/β-actin, fibronectin/β-actin, and E-cadherin/β-actin are shown. *C,* ChIP assay was performed on BEAS-2B cells treated with $NiCl_2$ for 48 h. The precipitated chromatin was PCR-amplified with the use of specific primers with E-boxes in the *E-cadherin* promoter. *In vivo* identification of reciprocal E-box occupancy by Snail or HIF-1α at the *E-cadherin* promoter in BEAS-2B cells was carried out. No antibodies were used as negative control. *Input*, PCRs performed on total chromatin from BEAS-2B cells. *Ab,* antibody.

cells (Fig. 5*B*), suggesting a partial role for HIF-1α in $NiCl_2$-mediated E-cadherin and fibronectin regulation.

Several transcriptional repressors, including Snail and Slug, are involved in the repression of E-cadherin expression (23). To assess whether $NiCl_2$ inhibits E-cadherin expression through these transcription factors, we evaluated the effect of $NiCl_2$ treatment on Snail and Slug expressions. As shown in Fig. 5*A*, cells exposed to $NiCl_2$ had higher Snail and Slug protein levels than untreated cells. Next, we performed ChIP assay to examine whether HIF-1α, Snail, and Slug transcription factors are responsible for *E-cadherin* promoter activity (−178 to +92). As shown in Fig. 5*C*, HIF-1α, Snail, and Slug were present on the *E-cadherin* promoter following $NiCl_2$ treatment, indicating that HIF-1α, Snail, and Slug are associated with $NiCl_2$-regulated E-cadherin reduction.

$NiCl_2$ Inhibits E-cadherin Expression Partly by Promoter Hypermethylation via ROS Generation—The regulation of *E-cadherin* gene expression in many biological processes involves epigenetic mechanisms, and aberrant methylation of *E-cadherin* correlates with transcriptional silencing of the gene in non-small cell lung cancer cells (24, 25). To examine whether $NiCl_2$ repression of E-cadherin is mediated by epigenetic effects, cells were pre(co)treated with 5-aza-2′-deoxycytidine (20 and 40 μM), a DNA methyltransferase inhibitor, and $NiCl_2$ at various concentrations for 48 h. It was found that 5-aza-2′-deoxycytidine restores E-cadherin expression following treatment with 0.25 mM $NiCl_2$ (Fig. 6*A*).

In an effort to facilitate the analysis of DNA samples isolated from BEAS-2B cells treated with $NiCl_2$, we used nested-PCR approach to study the methylation of the *E-cadherin* promoter. As shown in Fig. 6*B*, methylation of *E-cadherin* promoter increased following treatment with $NiCl_2$. To elucidate a link between ROS and DNA methylation, we examined whether the *E-cadherin* promoter methylation is altered by ROS. Nickel-induced methylation was blocked following treatment with NAC (Fig. 6*B*). The same results were obtained on QMSP assay of DNA methylation of E-cadherin. Treatment with 0.25 and 0.5 mM $NiCl_2$ caused 33.5-fold ($p < 0.01$) and 26.5-fold ($p < 0.01$) increases in E-cadherin methylation, respectively. Pretreatment with NAC significantly abolished nickel-induced *E-cadherin* hypermethylation (Fig. 6*C*). These data support the suppression of E-cadherin expression by $NiCl_2$-induced aberrant promoter methylation via ROS generation.

We also analyzed the methylation status of CpG islands at the *E-cadherin* promoter, including 29 CpG sites within a 349-bp fragment from sequence positions −211 to +138. Bisulfate sequencing analysis of five individual clones of each sample was carried out using PCR products from $NiCl_2$-treated BEAS-2B cells and lung cancer cell lines (A549, CL1-0, H1299, and H1355 cells). As shown in Fig. 7*A*, methylated CpG sites were more frequent in $NiCl_2$-treated BEAS-2B cells, especially at CpG site −56, when compared with untreated cells. Densely methylated clones were also detected in H1299 and H1355 cells (Fig. 7*B*). These results are consistent with the findings of our previous study that protein levels of E-cadherin are low in H1299 and H1355 cells (Fig. 2*F*). $NiCl_2$ contributes to the methylation of CpG islands on the *E-cadherin* promoter, resulting in decreased E-cadherin expression.

DISCUSSION

It has been well documented that nickel exposure leads to generation of ROS. Incremental levels of intracellular ROS, lipid peroxidation, hydroxyl radicals (OH•), and DNA damage

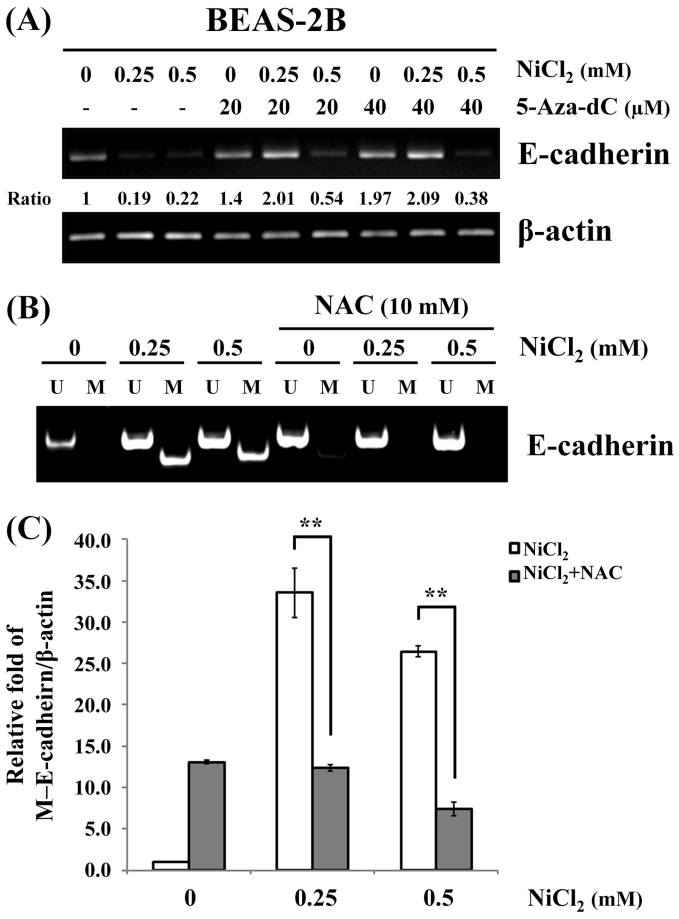

FIGURE 6. **Epigenetic effects of $NiCl_2$ down-regulate E-cadherin expression.** *A,* BEAS-2B cells were treated with $NiCl_2$ (0, 0.25, and 0.5 mM) and 5-Aza-dc (0, 20, and 40 μM) for 48 h. The mRNA levels of fibronectin and E-cadherin were determined by RT-PCR. β-Actin was used as the internal control. The relative ratios of E-cadherin/β-actin are shown. *B,* methylation-specific PCR assays were performed after BEAS-2B cells were pretreated with/without 10 mM NAC and then treated with $NiCl_2$ for 48 h. Visible PCR product in *lanes U* indicates the presence of unmethylated alleles; visible PCR product in *lanes M* indicates the presence of methylated alleles. *C,* QMSP analysis confirmed the same sample. DNA methylation of *E-cadherin* was calculated as the relative expression compared with β-actin. Each *bar* represents the mean ± S.D. of triplicate experiments. **, $p < 0.01$.

are induced in human lymphocytes after acute exposure to $NiCl_2$ (26). ROS are also enhanced in signal transduction events required for apoptosis under nickel exposure (27). Moreover, ROS are crucial conspirators in EMT engagement and tumor aggressiveness (28).

Nickel compounds are carcinogens that enhance invasion of human lung cancer cells (29, 30). In this study, $NiCl_2$ induced EMT phenotype marker alterations such as up-regulation of fibronectin and down-regulation of E-cadherin. Prolonged ROS stress by nickel stimulation down-regulated expression of E-cadherin via the HIF-1α-dependent pathway and DNA methylation. We addressed a novel aspect of lung carcinogenesis, specifically the transition to a stage of higher motility and thus progression of carcinogenesis. Nickel is potentially implicated in carcinogenesis via the production of ROS. Its potential to promote a migratory phenotype was investigated at the levels of gene and epigenetic modifications in EMT (Fig. 8).

We used NAC, Tiron, SOD, allopurinol, and rotenone to test our hypothesis that some ROS antioxidants or specific scavengers alleviate the EMT phenotype induced by $NiCl_2$. Both Tiron and SOD eliminated the superoxide anion and partially altered nickel-induced EMT signaling (Fig. 3*A*). Moreover, NOX1 increased in response to treatment with $NiCl_2$ (Fig. 4*C*). Knockdown of superoxide dismutase 2 genes did not restore the expression of E-cadherin (supplemental Fig. S2*B*), suggesting that superoxide is at least partly associated with nickel-induced EMT. The half-life of superoxide anion is short, and it rapidly dismutates either nonenzymically or via SOD to H_2O_2, which is relatively stable. NAC was found to be the best antioxidant for alleviating the EMT phenotype induced by $NiCl_2$ (Fig. 3*A*).

Hypochlorite anion (OCl^-) is a natural compound that forms from the reaction catalyzed by myeloperoxidase, an enzyme present only in innate immune cells (31). Both OCl^- and $OH^\bullet$ can be detected in photocatalytic ROS production using 3′-(*p*-aminophenyl) fluorescein. Monitoring of $OH^\bullet$ production using another fluorochrome called HPF suggested that nickel mainly induces $OH^\bullet$ generation (Fig. 4*A*). $OH^\bullet$ is produced with superoxide or H_2O_2. However, nickel did not affect the generation of superoxide anion (Fig. 4, *A* and *B*), which can also occur in the Haber-Weiss reaction by oxidation of the superoxide anion radical. In addition, we found that expressions of catalase and GPX1/2 decreased, whereas expression of SOD2 increased following nickel treatment (Fig. 4*C*), indicating that superoxide anions are barely detectable following nickel treatment. Moreover, in the presence of divalent metal ions such as Ni^{2+} and Fe^{2+}, H_2O_2 can undergo the Fenton reaction to produce $OH^\bullet$. The responses of BEAS-2B shSOD2 cells to nickel treatment were similar to those of BEAS-2B shLuc cells with EMT phenotype and superoxide generation (supplemental Fig. S2). H_2O_2 generation partly involves oxidases, SOD, and cytochrome P450 family of enzymes that are found in several subcellular compartments such as mitochondria, peroxisomes, and microsomes (32). Thus, the source of H_2O_2 by nickel production may be mediated through various pathways.

The most widely implemented application of JC-1 is for the detection of mitochondrial depolarization in the early stages of apoptosis. The effect of NAC on JC-1 monomer formation was highly unspecific as the readout doubled in the control and did not change regardless of nickel exposure (Fig. 4*D*). Similarly, the use of antioxidants, including NAC and penicillamine, induces apoptosis in multiple types of human cancer cells (33). The limitation of this study involves selection of optimal concentration of NAC to balance prevention of cytotoxicity and alleviation of EMT. EMT may be involved in multiple processes, and it is difficult to abolish the EMT phenotype by blockage of repressors for E-cadherin. Thus, multiple inhibitors might be helpful in lung cancer treatment.

Mutant P53 (R175H) induces Twist1 expression that is involved in the alleviation of epigenetic repression and EMT (34). Nickel may induce *p53* gene mutation and expression (35). Calcium signaling is required for EMT and E-cadherin silencing. In this study, 1,2-bis(2-aminophenoxy)ethane-*N*,*N*,*N*′,*N*′-tetraacetic acid tetrakis(acetoxymethyl ester) (BAPTA-AM) restored nickel-induced ROS generation (supplemental Fig. S3). Moreover, intracellular calcium may be involved in nickel-induced EMT. In this study, we used BEAS-2B cells, an immortalized lung bronchial epithelial cell line, to investigate metal

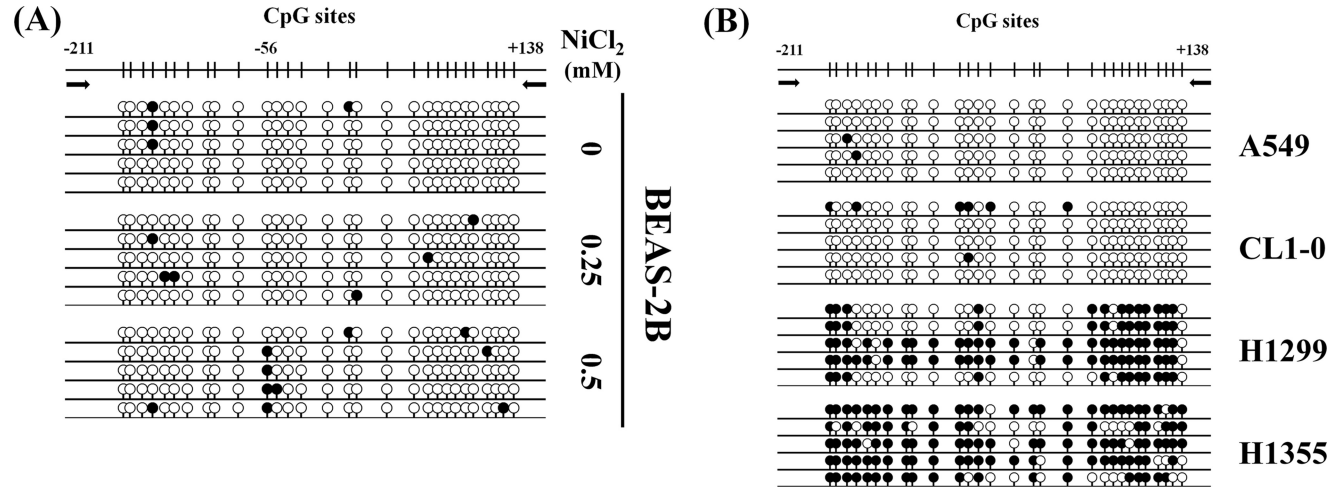

FIGURE 7. **Bisulfite genomic sequencing of *E-cadherin* promoter (−211 to +138).** Methylation status of CpG sites around the *E-cadherin* promoter region was analyzed in BEAS-2B cell line following treatment with $NiCl_2$ (0, 0.25, and 0.5 mM) (*A*) and lung cancer cell lines (A549, CL1-0, H1299, and H1355 cells) (*B*). Region spans −211 to +138 including 29 CpG sites. *Each row* represents an individual subclone. *White circles* represent unmethylated CpGs. *Black circles* represent methylated CpGs.

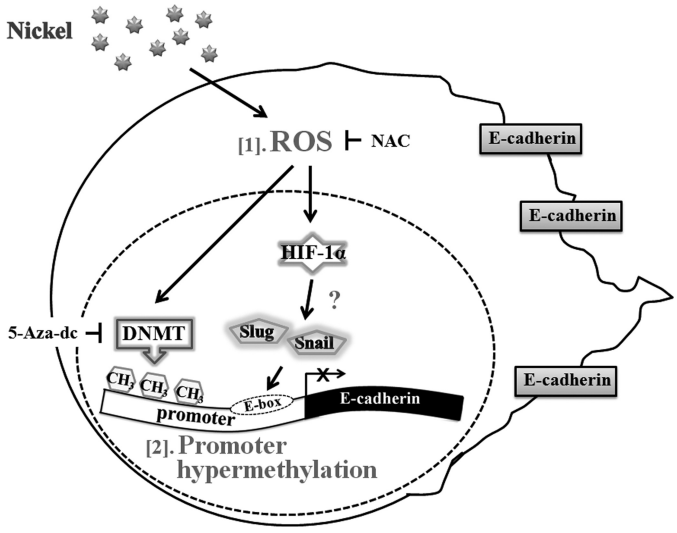

FIGURE 8. **Model depicting the mechanisms of nickel-repressed E-cadherin in BEAS-2B cells.** *[1]* nickel induces ROS generation and up-regulation of HIF-1α. *[2]* transcription factors, such as Snail and Slug, may be activated and inhibit expression of E-cadherin. Nickel represses E-cadherin by promoter hypermethylation via ROS generation.

compound-induced EMT. The data showed that metal compounds promote EMT, which may induce metastasis in early stage lung cancer.

HIF-1α has been shown to contribute to EMT through direct regulation of Twist expression, which inhibits E-cadherin transcription (36). Overexpression of HIF-1α induces EMT and promotes migration, invasion, and metastasis *in vitro* and *in vivo* (37), suggesting that HIF-1α is an important positive regulator of EMT. We observed induction of EMT by up-regulation of HIF-α following $NiCl_2$ treatment. In addition, knockdown of HIF-1α abolished EMT phenotype, providing further support for the role of HIF-1α in $NiCl_2$-induced EMT in BEAS-2B cells.

As shown in Figs. 5*C* and 6*C*, the results of ChIP and QMSP demonstrated that HIF-1α- and Snail-bound *E-cadherin* promoter regions contain methylated CpG sites in $NiCl_2$-treated cells. HIF-1α and Snail not only bind to but also induce DNA methylation of *E-cadherin* promoter, causing repression of transcription. Acute exposure to carcinogenic compounds of Ni(II) activates the transcription factor HIF-1α, which is associated with carcinogenesis, invasion, and angiogenesis (7, 36). A previous study has demonstrated that HIF-1α directly regulates the transcriptional repression of equilibrative nucleoside transporter during hypoxia (38). It has also been reported that HIF-1α acts in cooperation with other transcription factors and regulates target genes (39). Therefore, HIF-1α might directly mediate down-regulation of E-cadherin or cooperate with transcription repressors, such as Snail and Slug, to inhibit E-cadherin expression in $NiCl_2$-treated BEAS-2B cells. Further experiments are needed to prove our hypothesis.

Epigenetic alteration mechanisms, which include DNA hypermethylation and histone modifications, are involved in the regulation of gene expression. In addition, water-soluble nickel compounds can signal hypoxia (40). Silencing of seripina3g gene by nickel is partially reversed with trichostatin A (TSA) pretreatment (41). It is interesting to note that co-treatment with TSA does not affect down-regulation of E-cadherin by $NiCl_2$, suggesting that histone deacetylation is not involved in $NiCl_2$-repressed expression of E-cadherin (data not shown). Hypoxia and nickel exposure increase the level of H3K9me2 at the *Spry2* (*Sprouty homolog 2*) promoter by inhibiting histone demethylase JMJD1A, resulting in repression of *Spry2* in BEAS-2B cells (42). In addition to histone methylation, nickel can cause DNA hypermethylation (29). It has also been reported that inactivation of E-cadherin is the hallmark of tissue invasion and metastasis (43). Snail transcription factor represses the expression of E-cadherin by influencing transcription level and promoter hypermethylation. In hepatocellular carcinoma cells, ROS induces the hypermethylation of *E-cadherin* promoter via increasing Snail expression (44). Although down-regulation of E-cadherin by Snail through transcriptional inhibition could not be excluded, Snail might play an important role in $NiCl_2$-induced E-cadherin hypermethylation.

In conclusion, our data provided evidence that $NiCl_2$ promotes EMT. Persistently high levels of ROS stress trigger epigenetic changes in $NiCl_2$-treated cells. The results of this study showed that $NiCl_2$ induces EMT through a variety of mechanisms and provide novel insights into tumor progression by illustrating the association between $NiCl_2$ exposure and early lung cancer metastasis.

Acknowledgments—RNAi reagents were obtained from the National RNAi Core Facility (Institute of Molecular Biology/Genomic Research Center, Academia Sinica), which is supported by National Research Program for Genomic Medicine, National Science Council Grant NSC-97-3112-B-001-016. Confocal microscopy was performed by the Instrument Center of Chung Shan Medical University, which is supported in part by the National Science Council, Ministry of Education, and Chung Shan Medical University.

REFERENCES

1. Thiery, J. P. (2002) Epithelial-mesenchymal transitions in tumor progression. *Nat. Rev. Cancer* **2,** 442–454
2. Thiery, J. P., Acloque, H., Huang, R. Y., and Nieto, M. A. (2009) Epithelial-mesenchymal transitions in development and disease. *Cell* **139,** 871–890
3. Christiansen, J. J., and Rajasekaran, A. K. (2006) Reassessing epithelial to mesenchymal transition as a prerequisite for carcinoma invasion and metastasis. *Cancer Res.* **66,** 8319–8326
4. Kalluri, R. (2009) EMT. When epithelial cells decide to become mesenchymal like cells. *J. Clin. Invest.* **119,** 1417–1419
5. Thiery, J. P., and Sleeman, J. P. (2006) Complex networks orchestrate epithelial-mesenchymal transitions. *Nat. Rev. Mol. Cell Biol.* **7,** 131–142
6. Christofori, G., and Semb, H. (1999) The role of the cell-adhesion molecule E-cadherin as a tumor-suppressor gene. *Trends Biochem. Sci*. **24,** 73–76
7. Strathdee, G. (2002) Epigenetic *versus* genetic alterations in the inactivation of E-cadherin. *Semin. Cancer Biol*. **12,** 373–379
8. Chen, J., Imanaka, N., Chen, J., and Griffin, J. D. (2010) Hypoxia potentiates Notch signaling in breast cancer leading to decreased E-cadherin expression and increased cell migration and invasion. *Br. J. Cancer* **102,** 351–360
9. Veljkovic, E., Jiricny, J., Menigatti, M., Rehrauer, H., and Han, W. (2011) Chronic exposure to cigarette smoke condensate *in vitro* induces epithelial to mesenchymal transition-like changes in human bronchial epithelial cells, BEAS-2B. *Toxicol. In Vitro* **25,** 446–453
10. Galanis, A., Karapetsas, A., and Sandaltzopoulos, R. (2009) Metal-induced carcinogenesis, oxidative stress and hypoxia signaling. *Mutat. Res.* **674,** 31–35
11. Edelman, D. A., and Roggli, V. L. (1989) The accumulation of nickel in human lungs. *Environ. Health Perspect.* **81,** 221–224
12. Costa, M., Yan, Y., Zhao, D., and Salnikow, K. (2003) Molecular mechanisms of nickel carcinogenesis. Gene silencing by nickel delivery to the nucleus and gene activation/inactivation by nickel-induced cell signaling. *J. Environ. Monit.* **5,** 222–223
13. Hsin, I. L., Sheu, G. T., Chen, H. H., Chiu, L. Y., Wang, H. D., Chan, H. W., Hsu, C. P., and Ko, J. L. (2010) *N*-acetylcysteine mitigates curcumin-mediated telomerase inhibition through rescuing of Sp1 reduction in A549 cells. *Mutat. Res.* **688,** 72–77
14. Law, A. Y., Lai, K. P., Ip, C. K., Wong, A. S., Wagner, G. F., and Wong, C. K. (2008) Epigenetic and HIF-1 regulation of stanniocalcin-2 expression in human cancer cells. *Exp. Cell Res.* **314,** 1823–1830
15. Corn, P. G., Smith, B. D., Ruckdeschel, E. S., Douglas, D., Baylin, S. B., and Herman, J. G. (2000) E-cadherin expression is silenced by 5′ CpG island methylation in acute leukemia. *Clin. Cancer Res.* **6,** 4243–4248
16. Hiraki, M., Kitajima, Y., Sato, S., Mitsuno, M., Koga, Y., Nakamura, J., Hashiguchi, K., Noshiro, H., and Miyazaki, K. (2010) Aberrant gene methylation in the lymph nodes provides a possible marker for diagnosing micrometastasis in gastric cancer. *Ann. Surg. Oncol.* **17,** 1177–1186
17. Nojima, D., Nakajima, K., Li, L. C., Franks, J., Ribeiro-Filho, L., Ishii, N., and Dahiya, R. (2001) CpG methylation of promoter region inactivates E-cadherin gene in renal cell carcinoma. *Mol. Carcinog.* **32,** 19–27
18. Salnikow, K., and Costa, M. (2000) Epigenetic mechanisms of nickel carcinogenesis. *J. Environ. Pathol. Toxicol. Oncol.* **19,** 307–318
19. Davidson, T., Chen, H., Garrick, M. D., D'Angelo, G., and Costa, M. (2005) Soluble nickel interferes with cellular iron homeostasis. *Mol. Cell Biochem.* **279,** 157–162
20. Zhang, K. H., Tian, H. Y., Gao, X., Lei, W. W., Hu, Y., Wang, D. M., Pan, X. C., Yu, M. L., Xu, G. J., Zhao, F. K., and Song, J. G. (2009) Ferritin heavy chain-mediated iron homeostasis and subsequent increased reactive oxygen species production are essential for epithelial-mesenchymal transition. *Cancer Res.* **69,** 5340–5348
21. Galaris, D., and Evangelou, A. (2002) The role of oxidative stress in mechanisms of metal-induced carcinogenesis. *Crit. Rev. Oncol. Hematol.* **42,** 93–103
22. Gao, N., Shen, L., Zhang, Z., Leonard, S. S., He, H., Zhang, X. G., Shi, X., and Jiang, B. H. (2004) Arsenite induces HIF-1α and VEGF through PI3K, Akt, and reactive oxygen species in DU145 human prostate carcinoma cells. *Mol. Cell Biochem.* **255,** 33–45
23. de Herreros, A. G., Peiró, S., Nassour, M., and Savagner, P. (2010) Snail family regulation and epithelial mesenchymal transitions in breast cancer progression. *J. Mammary Gland Biol. Neoplasia* **15,** 135–147
24. Maeda, G., Chiba, T., Aoba, T., and Imai, K. (2007) Epigenetic inactivation of E-cadherin by promoter hypermethylation in oral carcinoma cells. *Odontology* **95,** 24–29
25. Kim, D. S., Kim, M. J., Lee, J. Y., Kim, Y. Z., Kim, E. J., and Park, J. Y. (2007) Aberrant methylation of E-cadherin and H-cadherin genes in non-small cell lung cancer and its relation to clinicopathologic features. *Cancer* **110,** 2785–2792
26. Chen, C. Y., Wang, Y. F., Huang, W. R., and Huang, Y. T. (2003) Nickel induces oxidative stress and genotoxicity in human lymphocytes. *Toxicol. Appl. Pharmacol*. **189,** 153–159
27. Patel, E., Lynch, C., Ruff, V., and Reynolds, M. (2012) Co-exposure to nickel and cobalt chloride enhances cytotoxicity and oxidative stress in human lung epithelial cells. *Toxicol. Appl. Pharmacol*. **258,** 367–375
28. Giannoni, E., Parri, M., and Chiarugi, P. (2012) EMT and oxidative stress. A bidirectional interplay affecting tumor malignancy. *Antioxid. Redox Signal* **16,** 1248–1263
29. Kasprzak, K. S., Sunderman, F. W., Jr., and Salnikow, K. (2003) Nickel carcinogenesis. *Mutat. Res*. **533,** 67–97
30. Xu, Z., Ren, T., Xiao, C., Li, H., and Wu, T. (2011) Nickel promotes the invasive potential of human lung cancer cells via TLR4/MyD88 signaling. *Toxicology* **285,** 25–30
31. Vladimirov, Y. A., and Proskurnina, E. V. (2009) Free radicals and cell chemiluminescence. *Biochemistry* (*Mosc.*) **74,** 1545–1566
32. Yeldandi, A. V., Rao, M. S., and Reddy, J. K. (2000) Hydrogen peroxide generation in peroxisome proliferator-induced oncogenesis. *Mutat. Res.* **448,** 159–177
33. Guan, D., Xu, Y., Yang, M., Wang, H., Wang, X., and Shen, Z. (2010) *N*-Acetylcysteine and penicillamine induce apoptosis via the ER stress response-signaling pathway. *Mol. Carcinog.* **49,** 68–74
34. Kogan-Sakin, I., Tabach, Y., Buganim, Y., Molchadsky, A., Solomon, H., Madar, S., Kamer, I., Stambolsky, P., Shelly, A., Goldfinger, N., Valsesia-Wittmann, S., Puisieux, A., Zundelevich, A., Gal-Yam, E. N., Avivi, C., Barshack, I., Brait, M., Sidransky, D., Domany, E., and Rotter, V. (2010) Mutant p53(R175H) up-regulates Twist1 expression and promotes epithelial-mesenchymal transition in immortalized prostate cells. *Cell Death Differ.* **18,** 271–281
35. Cameron, K. S., Buchner, V., and Tchounwou, P. B. (2011) Exploring the molecular mechanisms of nickel-induced genotoxicity and carcinogenicity. A literature review. *Rev. Environ. Health* **26,** 81–92
36. Yang, M. H., and Wu, K. J. (2008) TWIST activation by hypoxia inducible factor-1 (HIF-1). Implications in metastasis and development. *Cell Cycle* **7,** 2090–2096
37. Yang, M. H., Wu, M. Z., Chiou, S. H., Chen, P. M., Chang, S. Y., Liu, C. J., Teng, S. C., and Wu, K. J. (2008) Direct regulation of TWIST by HIF-1α

promotes metastasis. *Nat. Cell Biol.* **10,** 295–305
38. Eltzschig, H. K., Abdulla, P., Hoffman, E., Hamilton, K. E., Daniels, D., Schönfeld, C., Loffler, M., Reyes, G., Duszenko, M., Karhausen, J., Robinson, A., Westerman, K. A., Coe, I. R., and Colgan, S. P. (2005) HIF-1-dependent repression of equilibrative nucleoside transporter (ENT) in hypoxia. *J. Exp. Med.* **202,** 1493–1505
39. Warnecke, C., Zaborowska, Z., Kurreck, J., Erdmann, V. A., Frei, U., Wiesener, M., and Eckardt, K. U. (2004) Differentiating the functional role of hypoxia-inducible factor (HIF)-1alpha and HIF-2α (EPAS-1) by the use of RNA interference. erythropoietin is an HIF-2α target gene in Hep3B and Kelly cells. *FASEB J.* **18,** 1462–1464
40. Costa, M., Davidson, T. L., Chen, H., Ke, Q., Zhang, P., Yan, Y., Huang, C., and Kluz, T. (2005) Nickel carcinogenesis. Epigenetics and hypoxia signaling. *Mutat. Res.* **592,** 79–88
41. Zhao, J., Yan, Y., Salnikow, K., Kluz, T., and Costa, M. (2004) Nickel-induced down-regulation of serpin by hypoxic signaling. *Toxicol. Appl. Pharmacol.* **194,** 60–68
42. Chen, H., Kluz, T., Zhang, R., and Costa, M. (2010) Hypoxia and nickel inhibit histone demethylase JMJD1A and repress Spry2 expression in human bronchial epithelial BEAS-2B cells. *Carcinogenesis* **31,** 2136–2144
43. Hanahan, D., and Weinberg, R. A. (2000) The hallmarks of cancer. *Cell* **100,** 57–70
44. Lim, S. O., Gu, J. M., Kim, M. S., Kim, H. S., Park, Y. N., Park, C. K., Cho, J. W., Park, Y. M., and Jung, G. (2008) Epigenetic changes induced by reactive oxygen species in hepatocellular carcinoma. Methylation of the E-cadherin promoter. *Gastroenterology* **135,** 2128–2140